AGU ADVANCING EARTH AND SPACE SCIENCE

JGR Atmospheres

RESEARCH ARTICLE
10.1029/2020JD033384

Sensitivity of Grass Fires Burning in Marginal Conditions to Atmospheric Turbulence

Alexandra K. Jonko[1], **Kara M. Yedinak**[2,3,4], **Juliana L. Conley**[1,5], **and Rodman R. Linn**[1]

[1]Earth and Environmental Science Division, Los Alamos National Laboratory, Los Alamos, NM, USA, [2]University of Washington, School of Environmental and Forest Sciences, Seattle, WA, USA, [3]USDA Forest Service, Seattle, WA, USA, [4]USDA Forest Service, Forest Products Laboratory, Madison, WI, USA, [5]University of Rochester, Rochester, NY, USA

Key Points:

- Fires burning in marginal conditions are sensitive to small perturbations in the atmospheric flow field they are exposed to
- Ensemble simulations are necessary in order to fully capture not only the expected fire behavior but also the uncertainties associated with it

Correspondence to:

A. K. Jonko,
ajonko@lanl.gov

Citation:

Jonko, A. K., Yedinak, K. M., Conley, J. L., & Linn, R. R. (2021). Sensitivity of grass fires burning in marginal conditions to atmospheric turbulence. *Journal of Geophysical Research: Atmospheres*, *126*, e2020JD033384. https://doi.org/10.1029/2020JD033384

Received 30 JUN 2020
Accepted 1 JUN 2021

Author Contributions:

Conceptualization: Alexandra K. Jonko, Kara M. Yedinak, Rodman R. Linn
Data curation: Juliana L. Conley
Formal analysis: Alexandra K. Jonko, Kara M. Yedinak, Juliana L. Conley
Funding acquisition: Alexandra K. Jonko, Kara M. Yedinak
Investigation: Alexandra K. Jonko, Kara M. Yedinak, Juliana L. Conley
Methodology: Alexandra K. Jonko, Kara M. Yedinak, Rodman R. Linn
Project Administration: Alexandra K. Jonko
Software: Rodman R. Linn
Supervision: Kara M. Yedinak, Rodman R. Linn
Visualization: Alexandra K. Jonko
Writing – original draft: Alexandra K. Jonko, Kara M. Yedinak, Rodman R. Linn

Abstract Atmospheric forcing and interactions between the fire and atmosphere are primary drivers of wildland fire behavior. The atmosphere is known to be a chaotic system that, although deterministic, is very sensitive to small perturbations to initial conditions. We assume that as a result of the tight coupling between fire and atmosphere; wildland fire behavior, in turn, should also be sensitive to perturbations in atmospheric initial conditions. Observations suggest that low intensity prescribed fire, in particular, is susceptible to small perturbations in the wind field, which can significantly alter fire spread. Here, we employ a computational fluid dynamics model of coupled fire-atmosphere interactions to answer the question: How sensitive is fire behavior to small variations in atmospheric turbulence? We perform ensemble simulations of fires in homogenous grass fuels. The only difference between ensemble members is the state of the turbulent atmosphere provided to the model throughout the simulation. The atmospheric state is a function of the initial conditions applied at the start of the simulation and boundary conditions applied throughout the simulation. We find a wide range of outcomes, with area burned ranging from 2,212 to 11,236 m^2 (>400% change), driven primarily by sensitivity to initial conditions, with nonnegligible contributions from boundary condition variability during the initial 30 s of simulation. Our results highlight the need for ensemble simulations, especially when considering fire behavior in marginal burning conditions.

1. Introduction

An emerging challenge in wildland fire science is to understand and model the movement of prescribed fire. In 2019, almost 19 billion m^2 were burned in the United States by wildfire, compared with 25 billion m^2 burned using prescribed fire (National Interagency Fire Center, 2020). The area burned under prescription has increased from a 10 year average of 9.3 billion m^2, making up 57% of all burned area in 2000–2009, to 15 billion m^2, or 69% of all burned area in 2010–2019 (National Interagency Fire Center, 2020). It is clear that prescribed burning is a valuable tool of growing importance for land managers. It can be used to improve ecological health (Fitch & Kim, 2018; Knapp et al., 2009), protect vulnerable communities (Kolden & Henson, 2019; Mell et al., 2010), and reduce uncontrolled emissions from wildfires (Hyde et al., 2017; Schweizer & Cisneros, 2017; Ward & Lamb, 1970). At the same time, land managers and fire practitioners face a complex and variable coupled fire-atmosphere system that is modulated by a changing climate, dynamic ecosystems, and evolving management practices. Thus, when these decision-makers are evaluating the nature of their burning operation, they are navigating the largely unanalyzed nuances of a prescribed fire environment (Hiers, et al., 2020; Wonkka et al., 2015; Yedinak et al., 2018). Many processes, including the response of a smoke plume to the local atmospheric dynamics (Potter, 2012; Prichard et al., 2019) and the moisture response of fuel due to sun dappling below a canopy (Kreye et al., 2018) can influence a prescribed fire. Fire managers' ability to anticipate fire behavior is key to maximizing the social and ecological value of fire while simultaneously minimizing negative impacts (Hyde et al., 2017), and predictive models are critical to this task.

Prediction of fire behavior is complicated by the fact that small changes in environmental conditions can have large impacts on fire outcomes. The atmosphere is a chaotic system (Lorenz, 1963; Sivakumar, 2004; Zeng et al., 1993) which, although deterministic, is sensitive to small perturbations. When applying the governing equations to describe the motions of the atmosphere numerically, perturbations typically develop from initial and boundary conditions. Uncertainty in initial and boundary conditions stems from the fact that we have limited observations. In chaotic systems, small variations in initial and boundary conditions, which are frequently not reflected in the limited observations, can propagate and grow to have large effects on the solution to the equations. The chaotic nature of the atmosphere is the reason weather forecasts can only reliably be made for a limited number of days (Lorenz, 1969; Thompson, 1957; Tribbia & Baumhefner, 2004). Due to the coupling between fire and atmosphere, it is reasonable to assume that wildland fire behavior, in turn, should also be sensitive to small perturbations in atmospheric flow, or atmospheric turbulence (Holtslag, 2003). However, there is very limited literature investigating these relationships. Sun et al. (2009) were the first to show that fire area burned and rate of spread (*ROS*) are sensitive to atmospheric turbulence, as well as fire-induced variations in atmospheric flow using a large eddy simulation (LES) model coupled with an empirical fire spread model. Their results highlight the importance of including uncertainty estimates in fire behavior forecasts. During the 2012 RxCADRE prescribed-fire experiment, Clements et al. (2016) observed that fire spread for low-intensity prescribed fires was sensitive to small variations in wind speed and direction, corroborating these earlier results. They hypothesized that associated changes in fire spread could be a result of either fire-induced fire-atmosphere interactions or of the turbulence regime present at the time of ignition.

Process-based computational fluid dynamics models of wildfire (Sullivan, 2009), such as HIGRAD/FIRETEC (Linn, 1997; Linn et al., 2002), provide tools for exploring the characteristics of nonlinear interactions between fuels, terrain, and atmosphere. FIRETEC and similar CFD models are computationally very expensive. This means that often only a single simulation is carried out. However, when considering the chaotic dynamics of the atmosphere, an understanding of the influence of atmospheric variability on the outcomes of fires simulated by such models is needed. To establish confidence in any given forecast, it is a common practice in weather forecasting to perform ensemble model simulations and to consider the ensemble mean as well as the spread among ensemble members. Ensemble methods for weather forecasting were first suggested by Epstein (1969) and Leith (1974), and have been implemented since the 1990s (Houtekamer et al., 1996; Molteni et al., 1996).

Questions that arise when considering an appropriate modeling framework to investigate fire-atmosphere interactions include the following:

1. Is one simulation sufficient to capture system variability or is an ensemble approach needed?
2. Do some parameters influence the system variability more than the others do?
3. Are there relationships across parameters that further influence system variability?

These questions have not been explored in the context of process-based modeling of wildfire. However, as prescribed burning in marginal conditions has become a new application for process-based fire-atmosphere models (Furman et al., 2019; Hiers et al., 2020; Linn et al., 2021), these questions become more important to answer. Characterizing the sensitivity of model results to atmospheric turbulence will allow us to help optimize the implementation of process-based CFD modeling for application to prescribed fire research.

In this study, we test the hypothesis that fire behavior in marginal burning conditions, such as those used to conduct prescribed burns, is sensitive to small perturbations in atmospheric initial and boundary conditions using a physics-based fire behavior model. We use an ensemble approach to quantify the sensitivity of fire propagation to variability in the atmospheric flow field. Finally, we examine relationships between different aspects of the wind field and fire outcomes to identify the main drivers of sensitivity.

2. Methods

We use numerical simulations of an idealized fire burning in marginal conditions to investigate the impact of atmospheric turbulence on fire metrics including burnt area, rate of spread, and fuel consumption. Our analysis is carried out using HIGRAD/FIRETEC, a physics-based coupled fire-atmosphere model. We investigate the impact on an ensemble of fires of turbulent wind initial and boundary conditions.

2.1. Model Setup

HIGRAD/FIRETEC is a coupled fire-atmosphere model that combines a hydrodynamic model of atmospheric flow, HIGRAD (Reisner et al., 2000), with a combustion and heat transfer model, FIRETEC

(Linn, 1997; Linn et al., 2002; Pimont et al., 2009). HIGRAD is an atmospheric code that efficiently simulates flows on multiple time scales by splitting high-frequency phenomena from the governing equations. This is carried out by applying two nested time-stepping schemes. The results of the small time-stepping loop, which solves for fast-moving waves, are averaged and fed into the large time step, which solves the Navier-Stokes equations. This method enables HIGRAD to accurately capture strong gradients in temperature and velocity fields, such as those near and within a wildfire (Reisner et al., 2000). Sub-grid turbulence and aerodynamic drag associated with a three-dimensional volumetric representation of the vegetation are represented as a part of FIRETEC along with combustion and heat transfer. FIRETEC is based on the conservation of mass, momentum, species, and energy. The model employs a multiscale turbulence parameterization approach, including formulations for three fire-relevant size scales: s_A, the size of the largest fuel structures, s_B, associated with the distance between branches, and s_C, the size of small fuel structures, such as leaves and pine needles. Combustion is parameterized using a universal reaction rate, which is a function of fuel and oxygen density, turbulent intensity, the scale of the smallest fuel elements, and volume fraction of the resolved volume above critical ignition temperature (Linn, 1997). FIRETEC incorporates the macroscale effects (∼1–10 m) of combustion, radiation, convective heat transfer, and aerodynamic drag. A detailed description of the physical and chemical formulations of FIRETEC can be found in Linn (1997); Linn et al. (2002); Linn and Cunningham (2005) and Linn and Harlow (1998). FIRETEC has been developed to simulate wildfire, but its applicability to prescribed fire burning in marginal conditions has been evaluated against data collected during the 2012 RxCADRE fire experiment (Linn et al., 2021).

2.2. Simulations

Our core set of simulations (CORE) consists of an ensemble of 45 grass fires burning in marginal conditions. These simulations are essentially identical except that each fire is exposed to slightly different turbulent details of the initial and boundary wind conditions (the imposed mean wind profile is the same in all simulations). To isolate the effects of atmospheric turbulence on fire propagation, we simplify other components of the simulation setup as much as possible. To this end, we eliminate confounding impacts of vegetation structure and topography by using a homogenous surface fuel bed on a flat domain without topography. In most common grass fire simulations with FIRETEC (e.g., Cunningham & Linn, 2007; Linn & Cunningham, 2005), fuel beds are representative of Anderson Fuel Class 3 (Anderson, 1982) with a height of 0.7 m, and a fuel load of 0.7 kg m^{-2}, which is contained within the first grid cell above the surface. In such grass fire simulations, the surface area per unit volume of fuel is specified as 4,000 m^{-1}, which is typical for tall grass (e.g. Burgan, 1988; Rothermel, 1972), and the initial fuel moisture fraction (i.e., the mass of water divided by the mass of dry fuel) is usually set to 0.05. Since we are interested in marginal burning conditions, we increase the initial fuel moisture fraction to 0.2 (20% fuel moisture) and reduce the height of grass to 0.3 m. Fuel density within the fuel bed is kept the same, 1 kg m^{-3}, as in previous grass fire simulations, resulting in a fuel load in the surface grid cells of 0.3 kg m^{-2}. Computational domains for all fires have dimensions x = 400 m, y = 400 m, and z = 810 m. We use 2 m horizontal resolution, and a stretched vertical coordinate with an average resolution of 15 m, which translates to an effective resolution of 1.5 m near the surface and 50 m near the top of the domain. We employ a time step of 0.02 s or 50 Hz.

The turbulent wind initial and boundary conditions for fire ensemble simulations are obtained by performing a wind simulation using cyclic boundary conditions to capture the effects of a large fetch, which allows turbulence to spin-up. These wind spin-up simulations were performed on a domain that is much larger (x = 1,680 m, y = 1,680 m, and z = 810 m) than the domains used for fire simulations. The length scales of motion that are allowed to develop in a computational domain are essentially limited by the domain size. The rationale for this large-domain spin-up is to allow eddies to develop on length scales larger than the smaller domains in which fires are simulated, so as not to limit the size of turbulence by domain size. We initialize the wind field within the wind spin-up domain with a profile for the wind in the x-direction (u) that is empirically defined based on LAI and vegetation height (Kaimal & Finnigan, 1994; Raupach et al., 1996). The atmospheric stratification in all simulations is neutral, with an initial ambient temperature of 300 K. The streamwise velocity, u, varies between 0.5 m s^{-1} near the surface and 4.25 m s^{-1} at the top of the domain and is equal to 2.5 m s^{-1} at 10 m height, which is comparable with wind speeds observed during the 2012 RxCADRE (Linn et al., 2021). At $t = t_0$, we assume that cross-stream and vertical velocity, v and w, are zero

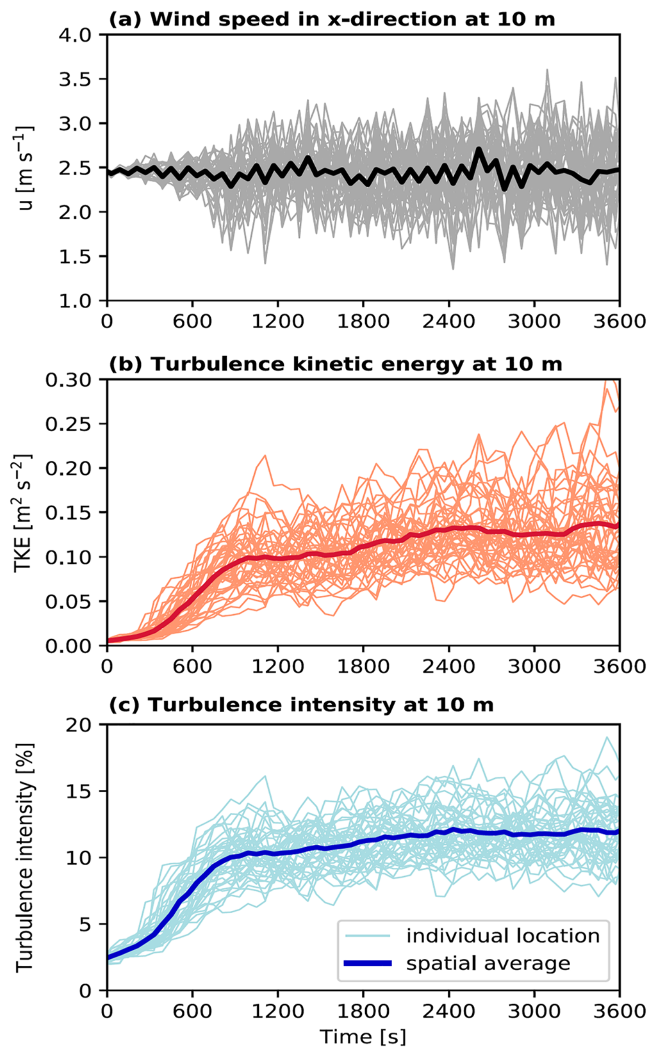

Figure 1. Characteristics of the wind field during spin-up sampled at 41 equally spaced locations across the large domain (thin lines) and their spatial average (thick lines). (a) Wind speed u in x-direction, (b) turbulence kinetic energy, and (c) turbulence intensity. All quantities are sampled at 10 m height above the surface.

everywhere. While in the real atmosphere sensible heat flux, a surface energy budget term related to diurnal solar forcing is a first-order driver of turbulence, surface heat fluxes are not represented in FIRETEC. The time scales simulated in FIRETEC are on the order of minutes to hours, and the diurnal cycle and associated variations in surface fluxes are not resolved. To ensure that turbulence develops efficiently in the spin-up simulation, we instead apply small random perturbations on the order of 0.1 K to the potential temperature in every grid cell throughout the domain at the beginning of the simulation. As the wind spin-up simulation progresses beyond $t = t_0$, turbulent motions develop in response to these initial perturbations. Vegetation drag continuously dissipates momentum in the domain. A dynamic macro-scale pressure gradient forcing is applied to compensate for this drag, enabling simulations of realistic wind fields (Pimont et al., 2018). We allow 60 min, which is equivalent to ~9 km of fetch, for turbulence to develop that is consistent with both upper-level winds and surface fuel structure. To verify that the turbulent wind field has reached steady state, we examine time series of *u* wind speed, turbulence kinetic energy (TKE), and turbulence intensity (Figure 1).

We consider domain averages of these quantities, as well as samples taken at 41 locations within the domain evenly spaced 100 m apart (at the centers and boundary intersections of the small fire simulation domains). These samples exhibit larger fluctuations than the domain average and are more directly comparable with observations, which would be collected at specific locations, rather than across a large area. After approximately 40 min, domain-average TKE and turbulence intensity have stopped increasing. Between 40 and 60 minutes, we observe low-frequency fluctuations around 0.13 m^2 s^{-2} for TKE and 12% for turbulence intensity. Note that the simulated TKE values are roughly an order of magnitude lower than the observations (Clements et al., 2008, 2016). This is primarily because the homogenous fuels used in this study have a very low surface roughness. Methods for generating stronger turbulence over homogenous fuels are the subject of ongoing research.

To ensure that our choice to use a large spin-up domain has the desired effect of allowing larger-scale turbulence to develop, we compare this spin-up to an analogous simulation run on a small domain with dimensions x = 400 m, y = 400 m, and z = 810 m. Figure 2 shows cross-stream spectra of *u* velocities at 10 m height for both simulations and highlights cross-stream variations at large length scales that are present in the large domain wind field, but absent from the small domain wind field. These larger-scale eddies can only be generated by using a large domain to spin-up the wind field.

After the 60 min spin-up, we begin saving initial and boundary conditions for nine adjacent subdomains with dimensions x = 400 m, y = 400 m, and z = 810 m, nested within the large domain (illustrated in Figure 3a). The wind spin-up yields nine sets of initial and boundary conditions (one for each subdomain), which were sampled from the large domain. Even though these nine sets of conditions were a part of the same large domain flow field, each had different instantaneous turbulent fluctuations as the turbulent conditions vary in space. To generate 45 simulations of fire with different turbulent conditions, we used the transient behavior of turbulent conditions in time. By choosing different moments in time to begin, fire simulations fires are exposed to different initial and boundary conditions. We selected five ignition times, 60 s apart, relative to the evolution of the large domain wind field. Since we are considering homogenous fuels and hold everything else the same, we use ignitions at different points in space and time relative to

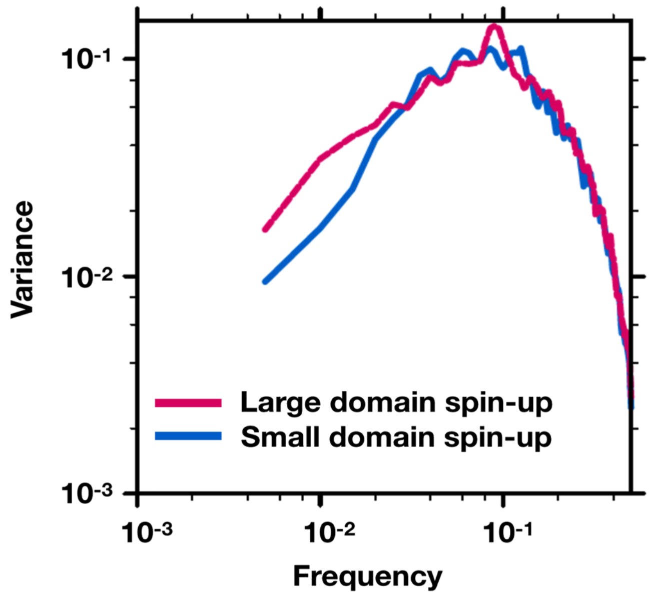

Figure 2. Comparison of wind spectra after spin-up using a large versus small domain. Cross-stream spectra for near-surface (10 m) wind in x-direction show differences at low frequencies, indicating that larger spatial scales of motion are absent when a small domain is used for spin-up (blue line). This cross-stream variance is present when a large spin-up domain is used (red line).

the turbulent wind field interchangeably. We use ignition lines that are 100 m long and 6 m deep, encompassing a total of 150 FIRETEC grid cells, which are ignited simultaneously.

The number of ensemble members for the CORE ensemble was chosen to ensure adequate sampling of the range of fire outcomes. To verify that we have chosen a sufficiently large number of members, we examine how the average and standard deviation of area burned evolve with the number of ensemble members. We begin with one member, and add members in increments of one until all 45 members are considered. Figure 3b shows that after the ensemble has reached 20 members, increasing the number does not significantly change the mean or standard deviation of the area burned.

In addition to the CORE set of simulations, we run two additional ensembles to disentangle the impact of initial conditions at the time of ignition from boundary conditions supplied throughout the simulation (Table 1). Initial conditions are provided at every grid point in the domain for the first time step of the simulation, while boundary conditions are imposed on the five lateral cells along the domain boundaries at every time step thereafter. Since fires generate their own turbulence, which can easily overpower background conditions, we assume that the boundary conditions post ignition provide a smaller perturbation when compared with the initial conditions, which are applied before and during ignition. To evaluate the importance of initial versus boundary conditions, we repeat simulations 2–21 of the core ensemble two more times. We choose 20-member ensembles based on our finding (shown in Figure 3b) because 20 ensemble members are needed to adequately sample the range of fire outcomes. In INIT simulations, we perturb the initial conditions as in the CORE ensemble (using initial conditions from CORE2 through CORE21), but use the same CORE1 boundary conditions for all simulations. In BOUND simulations, we use identical CORE1 full-domain initial conditions at the first time step for each ensemble member, but vary the boundary conditions along the course of the simulations

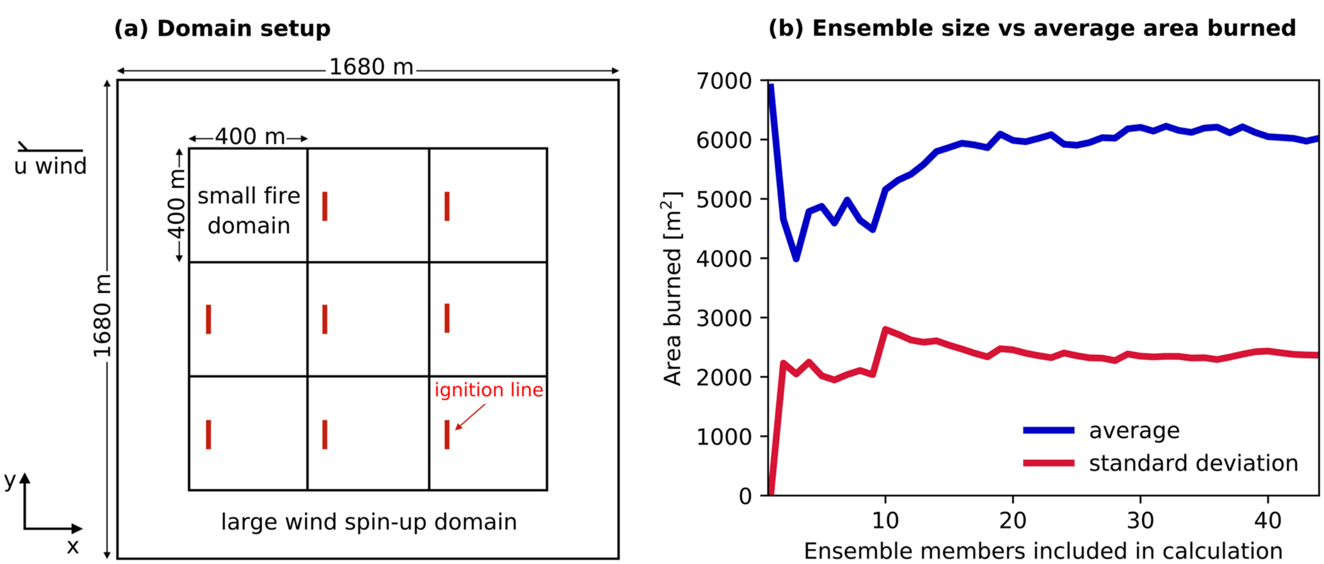

Figure 3. (a) The large 1,680 m by 1,680 m model domain used for wind spin-up in its center contains nine small 400 m by 400 m domains. Black lines are outlines of the domains, while red lines represent locations of ignition lines. A *u* wind in x-direction is prescribed. (b) Averages and standard deviations of area burned for an increasing number of ensemble members stabilize when at least 20 ensemble members are included, suggesting a minimum of 20 ensemble members are necessary to fully sample variability.

Table 1
Summary of Ensemble Simulations Performed

Ensemble name	Number of ensemble members	Description
CORE	45	Core simulations using homogenous grass fuels at 20% fuel moisture.
INIT	20	Initial conditions are perturbed as in CORE2-21, all simulations use CORE1 boundary conditions.
BOUND	20	Boundary conditions are perturbed as in CORE2-21, all simulations use CORE1 initial conditions.

in the same way as was carried out in the CORE ensemble (using CORE2-CORE21 boundary conditions). This setup is illustrated in Figure 4a for the first three domains that are part of INIT and BOUND ensembles. It allows us to ask the question of whether only the initial conditions – before/at ignition – matter, or whether the flow field provided to the model along the domain boundaries after ignition also plays a role. The effect on the wind field of perturbing only the initial versus only the boundary conditions is illustrated in Figures 4b and 4c. Figure 4b shows the difference in u wind speed at 10 m height along a cross-stream transect along the center of the domain between CORE1 and INIT3 wind-only (no fire) simulations, and its evolution over 300 s. The difference between CORE and INIT simulations stems from the fact that the two utilize different initial conditions. The simulations start out different—except along the domain boundaries, where identical boundary conditions are applied—but the differences fade over time. In some areas along the transect, differences approach zero as early as 80 s into the simulation, and they fade away entirely after 250 s. In Figure 4c, we examine the difference between CORE1 and BOUND3 wind-only simulations, which share initial conditions, but have different boundary conditions. The wind field is identical for the first 10 s, and differences begin to develop as boundary conditions propagate into the domain. After roughly 80 s, strong differences are present everywhere along the transect.

Because of the way ignition is handled in FIRETEC — the temperature of fuels along the ignition line is raised to an ignition temperature of 1,000 K over ~150 time steps, or three seconds — we start applying CORE2-CORE21 boundary conditions in BOUND simulations after the first 450 time steps.

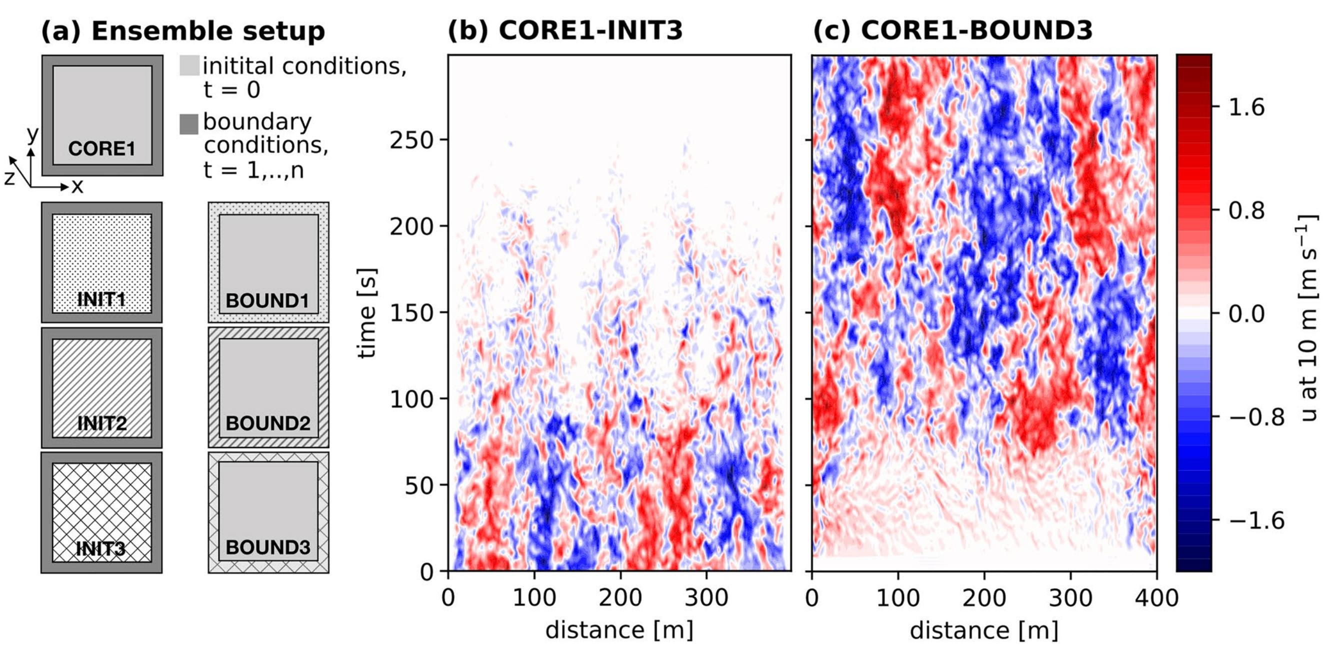

Figure 4. (a) Schematic of the setup of initial and boundary condition ensembles, shown for the first three of 20 ensemble members. Gray shading and textures are used interchangeably to denote different sets of conditions. (b)–(c) Evolution in time of differences between two wind-only (no fire) simulations representative of the core set of simulations (CORE) and initial conditions differ (INIT) ensembles (b), and the CORE and boundary conditions differ (BOUND) ensembles (c). u wind speeds at 10 m height are shown along a cross-stream transect over 300 s of simulation.

2.3. Analysis

The main goal of this study is to quantify the sensitivity of fire outcomes to small perturbations in the turbulent wind field in which the fires are exposed to. By using a homogenous fuel bed with constant fuel moisture, we attempt to eliminate factors that could complicate the interpretation of our results and assume that all differences between simulations within the same ensemble are solely due to the small differences in the turbulent wind field.

We use area burned, fire perimeter, fuel consumption, fire duration, rate of spread, and rate of growth as metrics to evaluate our results. Area burned, A (m^2) is calculated by summing the area of all cells from which more than 60% of fuel density has been removed through combustion. The fire perimeter is the outline of the area burned in meters. Consumption rate (or mass loss rate), C (kg s^{-1}) is computed as the difference in fuel density (kg m^{-3}) between adjacent time steps (s) multiplied by cell volume (m^3): $C = V\frac{\Delta\rho}{\Delta t}$. This metric is directly related to fire intensity, which can be obtained by multiplying C by the heat of combustion. We consider peak consumption, or the maximum value of consumption throughout the simulation, as well as the evolution of consumption with time. Fire duration, t_f, is calculated as the length of time (s) elapsed between ignition and the time when active consumption has stopped, defined as the time when solid fuel temperature in all computational cells drops below 400 K. *ROS* is the distance, d (m), of the fire front from the ignition line in the direction of the wind divided by t_f, while rate of growth (*ROG*) is the rate of change in area burned, or the area burned divided by t_f. To avoid folding the somewhat artificial model behavior during and immediately following ignition into the calculations for *ROS* and *ROG*, we start the calculations 100 s after ignition:

$$ROS = \frac{d(t_f) - d(100\text{s})}{t_f - 100\text{s}}$$

$$ROG = \frac{A(t_f) - A(100\text{s})}{t_f - 100\text{s}}$$

While *ROS* is a one-dimensional, directional measure of fire spread, which does not account for lateral spread, *ROG* is two-dimensional and considers forward as well as lateral spread into account.

Our analysis aims to determine which aspect of the wind perturbations is the dominant driver of variability in fire outcomes. To address this question, we examine correlations between the variability in fire metrics and different aspects of the wind field, including the mean wind in x, y, and z-direction, the resolved turbulent kinetic energy (TKE), and parameterized, sub-grid TKE in the CORE ensemble. We also examine the INIT and BOUND ensembles and compare them to simulations CORE2-21, to determine whether initial or boundary conditions play a larger role in driving variability in fire metrics.

3. Results

All simulations are run for 600 s of simulation time. We then assess whether the fire is still burning by examining gas temperature at the last time step. For all simulations, domain maximum values of gas temperature were below 400 K at 600 s and we assume that combustion has ceased. Even if pyrolysis is still occurring in small areas at this temperature, a return to more intense combustion and further spread of the fire is very unlikely.

3.1. Core Ensemble

In the 45-member CORE ensemble, the final area burned at the end of each simulation varies between 2,212 m^2 (CORE24) and 11,236 m^2 (CORE10), representing a 400% increase in area burned between the

Table 2
Summary of Fire Metrics for the CORE, INIT, and BOUND Ensembles

	CORE	CORE2-21	INIT	BOUND
$\overline{A}\ (m^2)$	6133.24	5991.40	4610.20	3579.20
CV_A	0.39	0.40	0.32	0.48
$\overline{P}\left(m\right)$	520.26	514.80	540.60	500.60
CV_P	0.14	0.16	0.14	0.16
$\overline{C_{peak}}\left(kg\ s^{-1}\right)$	1.73	1.70	1.39	1.07
$CV_{C_{peak}}$	0.35	0.38	0.28	0.46
$\overline{t_f}\left(s\right)$	446.02	434.50	432.00	427.00
CV_{t_f}	0.12	0.12	0.13	0.15
$\overline{ROS}\left(m\ s^{-1}\right)$	0.26	0.26	0.22	0.21
CV_{ROS}	0.20	0.20	0.38	0.46
$\overline{ROG}\left(m^2 s^{-1}\right)$	11.08	11.26	8.28	6.29
CV_{ROG}	0.44	0.43	0.38	0.59

Note. Ensemble averages are denoted by an overbar. Coefficients of variance (CV) are computed as the standard deviations normalized by the mean

smallest and largest fire. The average area burned across the ensemble is 6,133 m^2. We represent variation around the mean in terms of the coefficient of variance or standard deviation normalized by the mean. This allows us to compare variability across ensembles, and across metrics, which have means of different magnitude. The coefficient of variance for area burned in the CORE ensemble is 0.39 (see Table 2). Fire perimeters vary between 380 and 704 m, with an ensemble average of 520 m and a coefficient of variance of 0.15. Final burned areas for all 45 fires are shown in Figure 5 in terms of remaining fuel. While propagation occurs along the entire ignition line for some fires (e.g., domain 7, ignition at $t = 0$ s), other fires only spread from a subsection of the ignition line (e.g., domain 8, ignition at $t = 0$ s), or multiple portions of it (e.g., domain 5, ignition at $t = 0$ s). While some of the fires have a relatively "smooth" burned area, suggesting uniform spread (e.g., domain 2, ignition at $t = 180$ s), noticeable splitting of the fire front is evident in other burned areas (e.g., domain 3, ignition at $t = 60$ s, or domain 4, ignition at $t = 180$ s). Since the wind initial and boundary conditions are the only parameters that differ among these simulations, a multitude of fire behaviors can be attributed to only small perturbations in the wind field.

For each fire, we also consider the evolution of distance (*ROS*), area (*ROG*), and fuel consumption over time (Figure 6). Thin lines in Figure 6 represent individual CORE simulations, and the thick line is the ensemble mean. The top two panels show the range in distance from the ignition line and area burned over time. Lines crossing over each other indicate the range of spread and growth rates. The bottom panel tracks fuel consumption, highlighting a wide range of fire intensities. Peak consumption ranges between 0.66 kg s^{-1} for CORE2 and 2.91 kg s^{-1} for CORE10, with an average value of 1.73 kg s^{-1} and $CV_{C_{peak}} = 0.35$. We also observe large differences in the timing of peak consumption among the different fires. While CORE2 and CORE24 reach peak consumption after only 20 s, CORE29, which has the second-highest peak consumption at 2.76 kg s^{-1}, reaches this value only after 200 s. Fire duration ranges from 330 s for CORE9 to 588 s for CORE23, with an average of 446 s and $CV_{t_f} = 0.12$. The duration of the longest burning fire is thus only 80% longer than the shortest burning fire. This relatively smaller variability—characterized here in terms of the coefficient of variance across ensemble members—in fire duration compared with area burned is explained by different fire speeds, that is, the spread in *ROS* and *ROG*.

3.2. Initial and Boundary Condition Ensembles

We hypothesize that the variability induced by perturbing initial conditions at the time of ignition will be larger than the variability due to perturbing boundary conditions during the simulation. This is because fire-atmosphere feedbacks will induce atmospheric turbulence as the fire burns, which can overpower the small perturbations that we apply at the boundaries.

To test this hypothesis, we compare simulations CORE2-21 to two 20-member ensembles: one where only the initial conditions differ (INIT), and boundary conditions are the same for all 20 members and one where only boundary conditions differ (BOUND), while initial conditions are the same.

Average values and coefficients of variance for the different fire metrics are compared in Table 2, while Figure 7 shows time series of the distance of the fire front from the ignition line, the area burned, and fuel consumption. Overall, fires in both the INIT and BOUND ensembles are smaller, have lower peak consumption, slightly lower *ROS*, and significantly lower *ROG* than fires in the subset of the CORE ensemble. BOUND fires are generally smaller than INIT fires. They also have a shorter duration, and smaller perimeters, while the fire duration in the INIT ensemble is on par with the CORE ensemble subset, and INIT

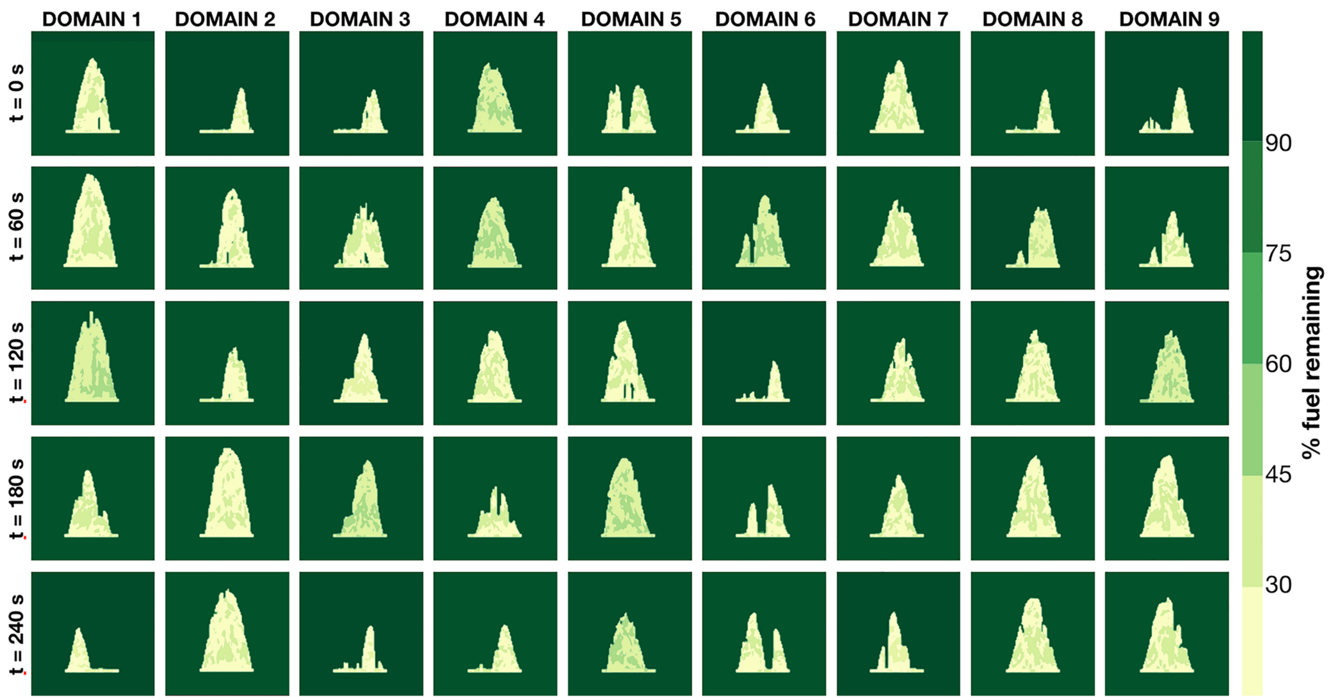

Figure 5. Final fire perimeters for the 45 fires in the core set of simulations (CORE) ensemble. Simulations are run in nine subdomains (columns) with five ignitions (rows) staggered in time for each subdomain.

perimeters are on average larger than CORE perimeters. Variability is larger in the BOUND ensemble than in the INIT or CORE2-21 ensembles for all metrics (compare the coefficient of variance in Table 2).

Figure 8 compares the degree of agreement between burned areas among the three ensembles. Some grid cells are burned by every fire in the ensemble and are assigned 100% agreement. If a fire is burned by only one of the 20 fires, it will have 5% agreement. The larger areas of low agreement in the BOUND ensemble (Figure 8c) confirm the results presented above. The overall smaller fire size is also apparent. These results do not confirm our hypothesis that fire behavior is influenced more by the state of the wind field close to ignition before the fire has gained significant momentum. Indeed, we find that the sustained perturbations applied along the domain boundary exert a large influence, possibly due to their duration, and the low-intensity nature of the fires we simulate.

We note that there is no relationship (quantified via r^2 values, which are < 0.1 for all cases), between the final area burned for the CORE, INIT, and BOUND ensembles, suggesting that nonlinear interactions between the boundary and initial conditions generate unique wind fields to which each fire is exposed, and which cannot be linearly decomposed into the influences of the initial and boundary conditions.

3.3. Attribution of Fire Variability to Atmospheric Perturbations

The variability we have characterized in Sections 3.1 and 3.2 is caused by differences in the atmospheric flow field imposed on each of the simulations. Next, we consider specifics of the wind field and their relationship to fire outcomes. We focus on final area burned in the CORE ensemble and correlate this metric with a series of characteristics of the atmospheric flow, including mean wind speed in x, y, and z-directions, fluctuations about the mean of wind speed in x, y, and z-directions, resolved and parameterized, and sub-grid TKE over different regions within the domain. Only mean x-direction (u) wind speed correlated significantly with the final area burned. Figure 9 shows r^2 values for regressions between u velocity averaged over different regions and area burned. Values below 0.5 are shown in blue, and r^2 values above 0.5 are shown in red. We use the F-test of overall significance to ensure that all correlations calculated here are statistically significant. The values in panel (a) are obtained by averaging u starting at the surface and along the ignition line, and growing the region vertically (one level at a time). The averaged area is incrementally

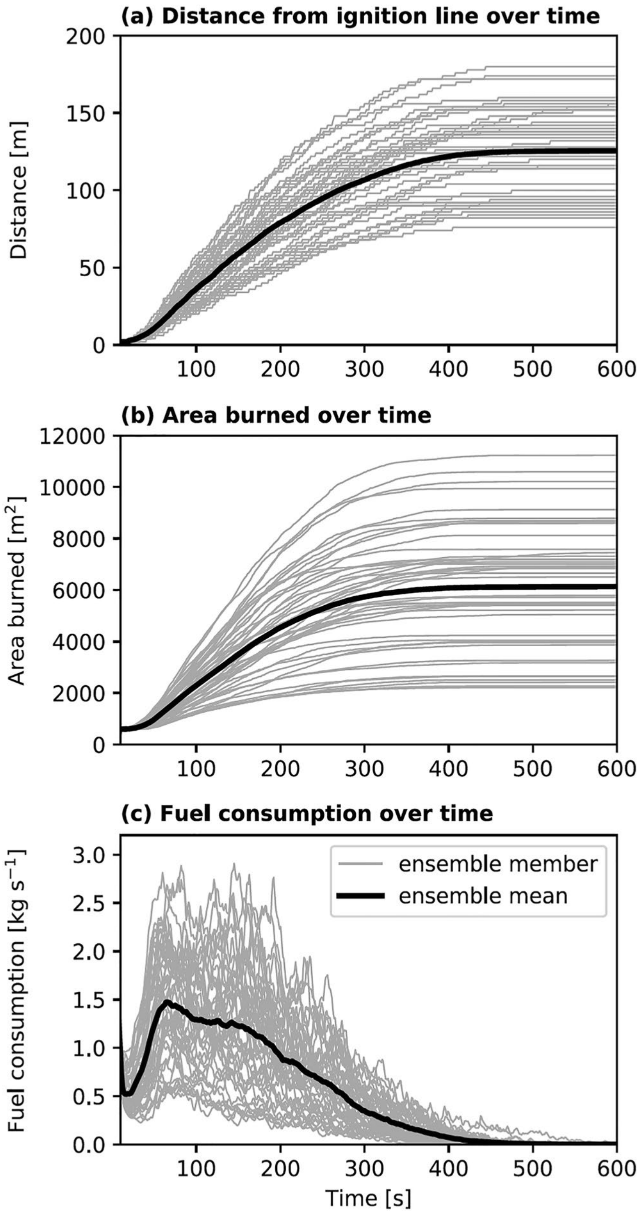

Figure 6. Evolution of fire propagation distance, area burned, and fuel consumption over time for the 45-member core set of simulations (CORE) ensemble.

moved away from the ignition line to assess locations upwind of the ignition. Each pixel value represents the r^2 value for that slice height and displacement from ignition. We see that the relationship between u and area burned grows stronger as the average expands farther upstream (closer to the inflow boundary). It also increases with height until the first 100 m and then decreases for averages including more vertical levels. In panel (b), we take a volume approach by averaging over incrementally larger vertical and horizontal ranges starting just upwind of the ignition line and working backward and upwards to the inflow boundary. The pixel location and associated value mark the furthest extent of the averaged volume from the ignition and associated r^2 value. We do this to assess whether the high positive r^2 values obtained when we average over a vertical slice between the ignition line and the inflow boundary are related to an entire atmospheric slab, or whether sections of this slab play a dominant role. r^2 values are generally lower when averaging over volumes, and $r^2 > 0.5$ values are concentrated near the inflow boundary. This tells us that u wind speeds at heights between 20 and 100 m at the inflow boundary drive the positive relationship with area burned. The u averages considered in panels (a) and (b) were taken just before the time of ignition. Since boundary conditions after ignition likely impact variability in area burned as well, we repeat the regression analysis throughout the simulation. We focus on the center of the five cells along the inflow boundary, where boundary conditions from the wind spin-up are passed into the domain, and average over increasing numbers of vertical levels. Results are shown in panel (c), which illustrates that boundary conditions influence fire outcomes only during the first 30 s of simulation after ignition has taken place.

This is likely the most sensitive time for fire development in our model—after the artificial ignition process, but before fire intensity has reached a level of generating sufficient buoyancy to dominate the local turbulence in its vicinity, locally overpowering the ambient wind fluctuations and thus becoming more self-determining.

It is important to note that the specifics of these results are likely sensitive to our choice of ignition line distance from the inflow boundary, as well as the mean wind speed. Both of these factors influence how long it takes for boundary conditions to reach the vicinity of the fire. When the ignition line is located farther downstream, we anticipate the boundary conditions to have a much smaller influence overall since more time would have to pass before the impact of the boundary conditions reached the fire itself. This increases the likelihood that the fire would have developed self-determining behavior before it is exposed to the impact of boundary conditions. When the ignition line is closer to the inflow boundary, however, we may see an increased influence of boundary conditions. A lower or higher mean wind speed might impact the sensitivity of fire to boundary conditions in an analogous way, with faster wind speeds leading to the fire being exposed to boundary conditions earlier in its propagation, and vice versa.

4. Conclusions

This study has quantified the sensitivity of fire behavior to atmospheric conditions for the first time using a computational fluid dynamics model of fire-atmosphere interactions. We find that low-intensity grass fires burning in marginal conditions in the fire behavior model FIRETEC are susceptible to small

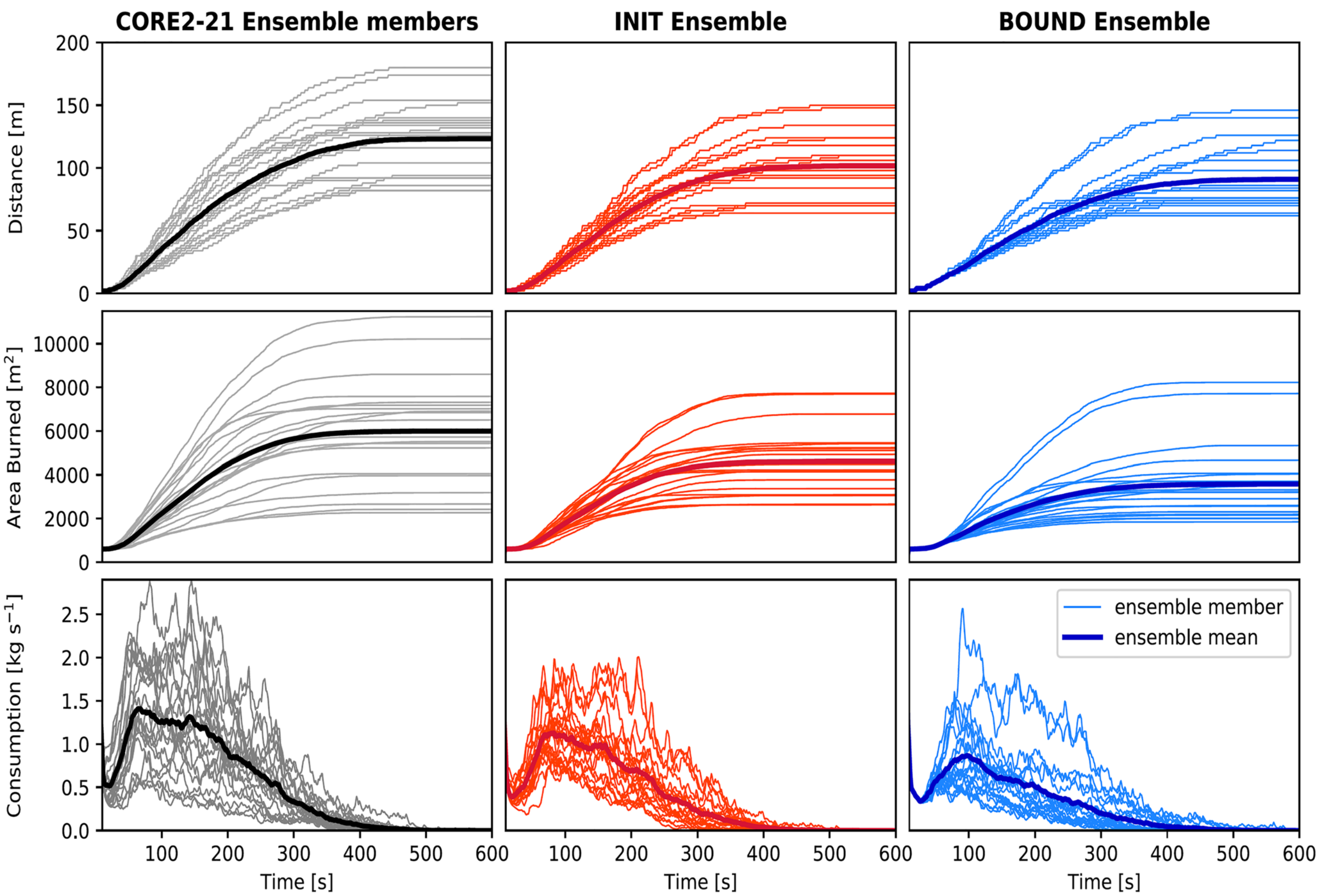

Figure 7. Evolution over time of propagation distance, area burned, and fuel consumption for the 20 members of the initial conditions differ (INIT) and boundary conditions differ (BOUND) ensembles, compared to members 2–21 of the core set of simulations (CORE) ensemble.

perturbations in the turbulent atmospheric flow field. Area burned and fuel consumption in the core ensemble of simulations varied by over 400%, from 2,212 to 11,236 m^2 and from 478 to 2,401 kg, respectively. Fire duration varied by 80%, from 330 to 590 s.

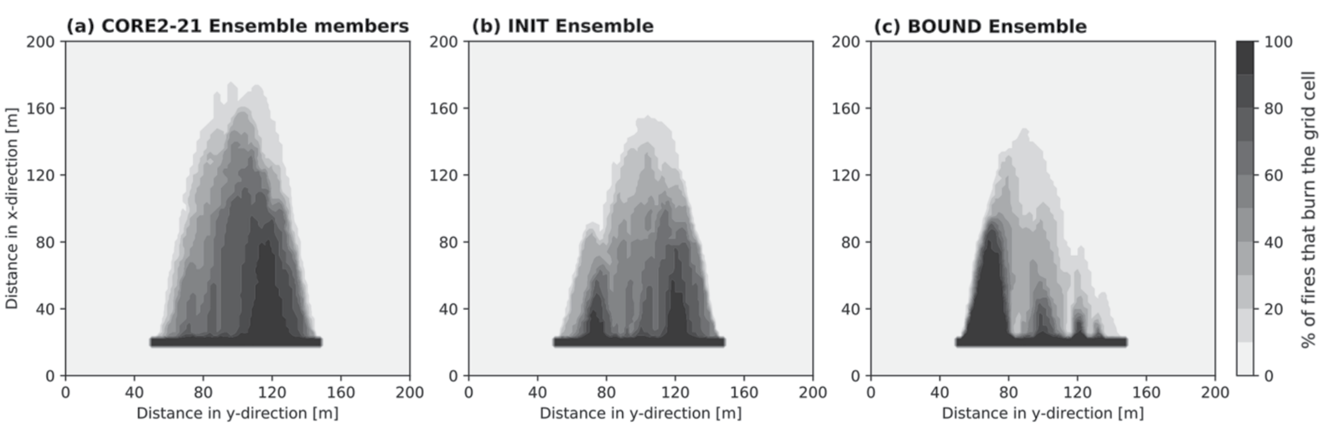

Figure 8. Percent of fire simulations in which any given grid cell is burned; defined as ≥60% of fuel being consumed. (a) shows the degree of agreement among the burned areas for members 2–21 of the core set of simulations (CORE) ensemble, (b) shows the initial conditions differ (INIT) ensemble, and (c) the boundary conditions differ (BOUND) ensemble. Areas that were burned by all fires are in black (100% agreement). Large areas with low percentages indicate more variability in the shape of burned areas. While the fire perimeters are generally smaller for the BOUND ensemble, we also find more variability in fire shapes than in the CORE and INIT ensembles.

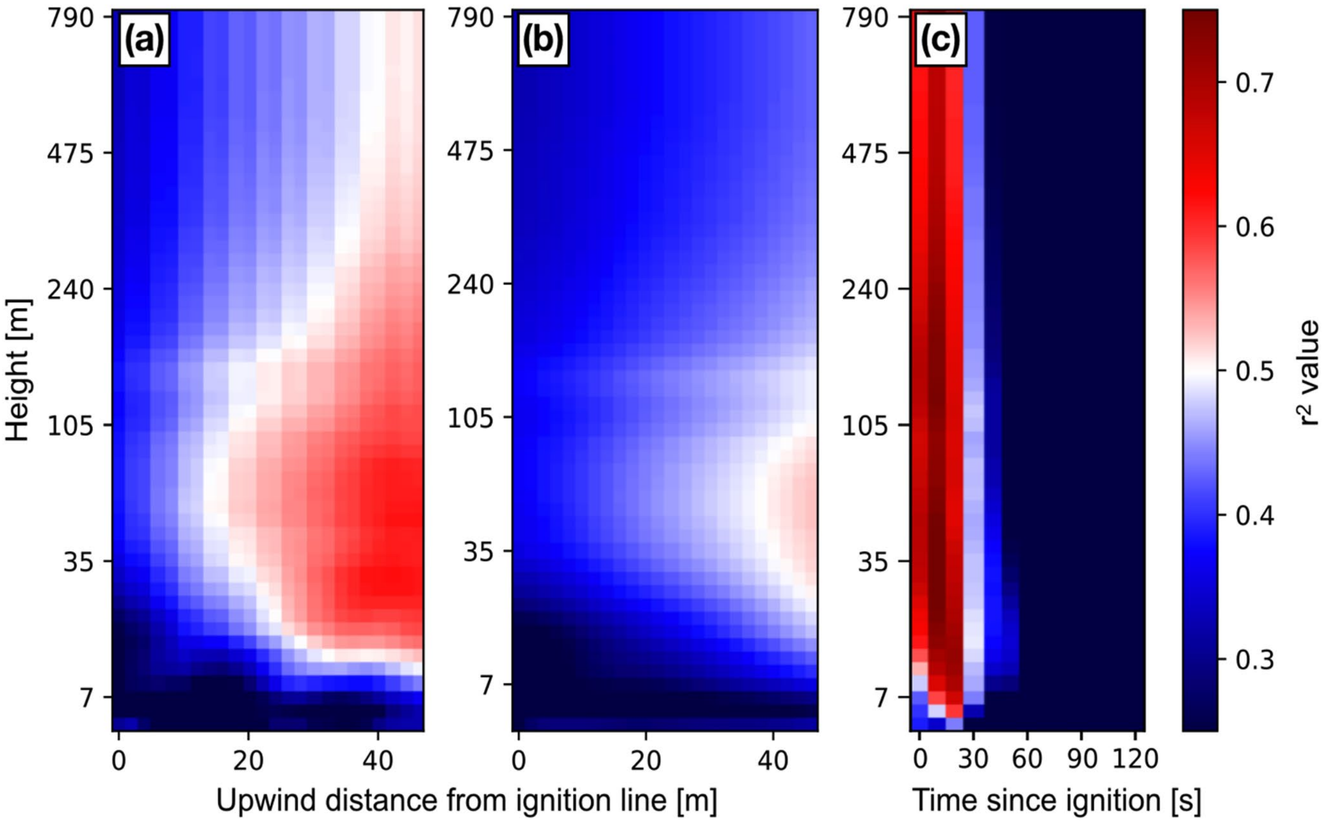

Figure 9. r^2 values characterizing relationships between final area burned and u wind speed averaged over different areas and for different times since ignition. (a) u is averaged vertically and moving backward from the ignition line to the inflow boundary. (b) u is averaged across a volume that grows vertically and horizontally from the ignition line to the inflow boundary. (c) Vertical average at inflow boundary of u at different times since ignition. Results suggest a relationship between variability in final area burned and the wind speed near the inlet boundary at the time of ignition and up to 30 s afterward.

This sensitivity has been previously suggested based on field observations during prescribed fires (Clements et al., 2016). We identify variability in mean along-stream wind speed at the inflow boundary of the model domain just before ignition and during the initial 30 s following ignition as the main driver of the variability in fire outcomes.

Turbulent wind conditions are introduced to the fire simulations in the form of initial conditions applied throughout the atmosphere at the first time step of the simulations, and boundary conditions applied throughout the simulations along the lateral domain boundaries. We find that fire propagation is more sensitive to boundary conditions, although we also detect nonnegligible sensitivity to initial conditions. Based on the results of our correlation analysis, the influence of boundary conditions is limited to the first 30 s after ignition.

In this study, we have mapped a small portion of the uncertainties inherent in FIRETEC simulations. We have considered uncertainty introduced through atmospheric initial and boundary conditions. There are many more parameters in FIRETEC that we have not considered in this idealized model setup. While mapping the entire uncertainty space of a complex model such as FIRETEC would be a massive undertaking beyond the scope of this study, we want to highlight the two factors we believe are particularly important and will be addressed in future work. First, we have excluded the impact of fuel heterogeneity by focusing on homogeneous grass in our study. However, we expect that nonlinear relationships exist between the heterogeneity of the wind field and fuel arrangement, which will impact the relationships we have identified here. We also expect that the relationships between the fire metrics we have chosen and wind variability will be sensitive to variations in fuel moisture. Anecdotal observations from managers indicate that fire spread and intensity decrease with increasing fuel moisture and in turn leave the fire more sensitive to wind perturbations. Thus, while prescribed fires in higher fuel moisture conditions burn more slowly and less intensely, they also have the potential to be less predictable. Future work will address this, as well as the influence of fuel heterogeneity.

More broadly speaking, low-intensity prescribed fires are known to be sensitive to factors not considered in our study, including the measurable response of prescribed fires to changes in environmental parameters such as the diurnal variability of fuel moisture (Anderson, 1990; Dahale et al., 2013; Jolly, 2007; Kreye et al., 2018), the influence of local atmospheric stability (Nelson, 2003; Reifsnyder, 1954; Reisner et al., 2000), or vertical wind shear (Kochanski et al., 2013), the spatial distribution of vegetation (Gagnon et al., 2012; Hiers et al., 2009; Kerby et al., 2007; O'Brien et al., 2016), and heterogeneous species combinations (Loudermilk et al., 2014; Thaxton & Platt, 2006). Future explorations of these sensitivities will allow us to develop a deeper understanding of the mechanisms and scales of influence across wildland fire scenarios.

Finally, we would like to call for attention to the need for an evolution in shape analysis in wildland fire research from a qualitative bulk-properties assessment to a quantitative approach. Our research highlights a large range of variability in burned area morphologies. The metrics currently in use in fire science, such as burn area, fire perimeter, and fire-line depth, do not sufficiently capture the detailed nature of the dynamic development of burned area morphologies. Different morphometry approaches exist in other disciplines, including botany (Belcher, 2016; Chuanromanee et al., 2019; Klein & Svoboda, 2017; Viscosi & Cardini, 2011), geomorphology (Cannon & Gartner, 2007; Whitten & Martin, 2019; Zhao et al., 2020), and medical research (Chollet et al., 2014; Claes et al., 2012; Mitteroecker et al., 2013). These approaches were designed for different physical systems and are not directly applicable to capturing details specific to fire behavior. Toward that goal, we are currently developing morphometric methods specifically for wildfire applications.

We set out to test the hypothesis that low-intensity fires burning in marginal conditions (e.g., prescribed fires) are sensitive to small perturbations in the atmospheric flow field. We found significant sensitivity of area burned and fuel consumption to small variations in the turbulent atmosphere around the time of ignition and for a short time afterward. Our results emphasize the need for ensemble simulations, and highlight the predictive limitations of individual fire simulations, particularly when it comes to prescribed fire.

Conflict of Interest

The authors declare no conflicts of interest.

Data Availability Statement

Data used to generate Figures presented in this study can be accessed at https://doi.org/10.5281/zenodo.4762971.

Acknowledgments

The authors have benefitted greatly in formulating the ideas in this paper from enjoyable discussions with Adam Atchley, Russell Parsons, Francois Pimont, Brian Potter, and Larry Pierce. This research was supported by the Los Alamos National Laboratory (LANL) through its Center for Space and Earth Science (CSES), and through LANL's Laboratory Directed Research and Development (LDRD) program under project number 20190310ER. CSES is funded by LDRD under project number 20180475DR. This research used resources provided by the Los Alamos National Laboratory Institutional Computing Program, which is supported by the U.S. Department of Energy National Nuclear Security Administration under Contract DE-AC52-06NA25396. K. Yedinak acknowledges support from the USDA Forest Service Pacific Northwest Research Station and the University of Washington.

References

Anderson, H. E. (1982). *Aids to determining fuel models for estimating fire behavior*. Ogden, UT: United Stated Department of Agriculture Forest Service.

Anderson, H. E. (1990). Moisture diffusivity and response time in fine forest fuels. *Canadian Journal of Forest Research*, *20*(3), 315–325. https://doi.org/10.1139/x90-046

Belcher, C. M. (2016). The influence of leaf morphology on litter flammability and its utility for interpreting palaeofire. *Philosophical Transactions of the Royal Society B: Biological Sciences*, *371*(1696), 20150163. https://doi.org/10.1098/rstb.2015.0163

Burgan, R. E. (1988). *1988 revisions to the 1978 national fire-danger rating system* (pp. 39). U.S. Department of Agriculture, Forest Service. Research Paper INT USA. SE-273.

Cannon, S. H., & Gartner, J. E. (2007). Wildfire-related debris flow from a hazards perspective. In *Debris-flow hazards and related phenomena* (pp. 363–385). Springer Berlin Heidelberg. https://doi.org/10.1007/3-540-27129-5_15

Chollet, M. B., Aldridge, K., Pangborn, N., Weinberg, S. M., & DeLeon, V. B. (2014). Landmarking the brain for geometric morphometric analysis: An error study. *PloS One*, *9*(1), e86005. https://doi.org/10.1371/journal.pone.0086005

Chuanromanee, T. S., Cohen, J. I., & Ryan, G. L. (2019). Morphological analysis of size and shape (MASS): An integrative software program for morphometric analyses of leaves. *Applications in Plant Sciences*, *7*(9), e11288. https://doi.org/10.1002/aps3.11288

Claes, P., Daniels, K., Walters, M., Clement, J., Vandermeulen, D., & Suetens, P. (2012). Dysmorphometrics: The modelling of morphological abnormalities. *Theoretical Biology and Medical Modelling*, *9*(1), 5. https://doi.org/10.1186/1742-4682-9-5

Clements, C. B., Lareau, N. P., Seto, D., Contezac, J., Davis, B., Teske, C., et al. (2016). Fire weather conditions and fire–atmosphere interactions observed during low-intensity prescribed fires – RxCADRE 2012. *International Journal of Wildland Fire*, *25*, 90–101. https://doi.org/10.1071/WF14173

Clements, C. B., Zhong, S., Bian, X., Heilman, W. E., & Byun, D. W. (2008). First observations of turbulence generated by grass fires. *Journal of Geophysical Research*, *113*(D22), D22102. https://doi.org/10.1029/2008JD010014

Cunningham, P., & Linn, R. R. (2007). Numerical simulations of grass fires using a coupled atmosphere-fire model: Dynamics of fire spread. *Journal of Geophysical Research*, *112*(D5), D05108. https://doi.org/10.1029/2006JD007638

Dahale, A., Ferguson, S., Shotorban, B., & Mahalingam, S. (2013). Effects of distribution of bulk density and moisture content on shrub fires. *International Journal of Wildland Fire*, *22*(5), 625–641. https://doi.org/10.1071/WF12040

Epstein, E. S. (1969). Stochastic dynamic prediction. *Tellus*, *21*(6), 739–759. https://doi.org/10.3402/tellusa.v21i6.10143

Fitch, R. A., & Kim, Y. S. (2018). Incorporating ecosystem health and fire resilience within the unified economic model of fire program analysis. *Ecological Economics*, *149*, 98–104. https://doi.org/10.1016/j.ecolecon.2018.02.017

Furman, J., Linn, R. R., Williams, B., & Winterkamp, J. (2019). *ESTCP project RC-201303: Using a computational fluid dynamics model to guide wildland fire management*. DoD SERDP-ESTCP project report.

Gagnon, P. R., Harms, K. E., Platt, W. J., Passmore, H. A., & Myers, J. A. (2012). Small-scale variation in fuel loads differentially affects two co-dominant bunchgrasses in a species-rich pine savanna. *PloS One*, *7*(1), e29674. https://doi.org/10.1371/journal.pone.0029674

Hiers, J. K., O'Brien, J. J., Mitchell, R. J., Grego, J. M., & Loudermilk, E. L. (2009). The wildland fuel cell concept: an approach to characterize fine-scale variation in fuels and fire in frequently burned longleaf pine forests. *International Journal of Wildland Fire*, *18*(3), 315–325. https://doi.org/10.1071/WF08084

Hiers, J. K., O'Brien, J. J., Varner, J. M., Butler, B. W., Dickinson, M., Hood, S. M., et al. (2020). Prescribed fire science: The case for a refined research agenda. *Fire Ecology*, *16*, 11. https://doi.org/10.1186/s42408-020-0070-8

Holtslag, A. A. M. (2003). Atmospheric turbulence. In R. A. Meyers (Ed.), *Encyclopedia of physical science and technology* (pp. 707–719). Elsevier Science Ltd. https://doi.org/10.2514/3.50485

Houtekamer, P. L., Lefaivre, L., Derome, J., Ritchie, H., Mitchell, H. L., Houtekamer, P. L., et al. (1996). A system simulation approach to ensemble prediction. *Monthly Weather Review*, *124*, 1225–1242. https://doi.org/10.1175/1520-0493

Hyde, J. C., Yedinak, K. M., Talhelm, A. F., Smith, A. M. S., Bowman, D. M. J. S., Johnston, F. H., et al. (2017). Air quality policy and fire management responses addressing smoke from wildland fires in the United States and Australia. *International Journal of Wildland Fire*, *26*, 347–363. https://doi.org/10.1071/WF16154

Jolly, W. M. (2007). Sensitivity of a surface fire spread model and associated fire behaviour fuel models to changes in live fuel moisture. *International Journal of Wildland Fire*, *16*(4), 503–509. https://doi.org/10.1071/WF06077

Kaimal, J. C., & Finnigan, J. J. (1994). *Atmospheric boundary layer flows: Their structure and measurement*. New York, NY: Oxford University Press.

Kerby, J. D., Fuhlendorf, S. D., & Engle, D. M. (2007). Landscape heterogeneity and fire behavior: Scale-dependent feedback between fire and grazing processes. *Landscape Ecology*, *22*(4), 507–516. https://doi.org/10.1007/s10980-006-9039-5

Klein, L., & Svoboda, H. (2017). Comprehensive methods for leaf geometric morphometric analyses. *Bio-Protocol*, *7*(9), 1–21. https://doi.org/10.21769/bioprotoc.2269

Knapp, E., Estes, B., & Skinner, C. (2009). *Ecological effects of prescribed fire season: A literature review and synthesis for managers*. JFSP Synthesis Reports.

Kochanski, A., Jenkins, M. A., Sun, R., Krueger, S., Abedi, S., & Charney, J. (2013). The importance of low-level environmental vertical wind shear to wildfire propagation: Proof of concept. *Journal of Geophysical Research: Atmosphere*, *118*(15), 8238–8252. https://doi.org/10.1002/jgrd.50436

Kolden, C. A., & Henson, C. (2019). A socio-ecological approach to mitigating wildfire vulnerability in the wildland urban interface: A case study from the 2017 Thomas fire. *Fire*, *2*(1), 9. https://doi.org/10.3390/fire2010009

Kreye, J. K., Hiers, J. K., Varner, J. M., Hornsby, B., Drukker, S., & O'brien, J. J. (2018). Effects of solar heating on the moisture dynamics of forest floor litter in humid environments: Composition, structure, and position matter. *Canadian Journal of Forest Research*, *48*(11), 1331–1342. https://doi.org/10.1139/cjfr-2018-0147

Leith, C. E. (1974). Theoretical skill of monte carlo forecasts. *Monthly Weather Review*, *102*, 409–418. https://doi.org/10.1175/1520-0493(1974)102

Linn, R., Winterkamp, J., Furman, J., Williams, B., Hiers, J. K., Jonko, A., et al. (2021). Modeling low intensity fires: Lessons learned from 2012 RxCADRE. *MDPI Atmosphere*, *12*, 139. https://doi.org/10.3390/atmos12020139

Linn, R. R. (1997). Doctoral Thesis*A transport model for prediction of wildfire behavior*. Las Cruces, NM: New Mexico State University.

Linn, R. R., & Cunningham, P. (2005). Numerical simulations of grass fires using a coupled atmosphere–fire model: Basic fire behavior and dependence on wind speed. *Journal of Geophysical Research*, *110*, D13107. https://doi.org/10.1029/2004JD005597

Linn, R. R., & Harlow, F. H. (1998). Mixing-limited transport model used for description of wildfires. In C. R. Kleijn, S. Kawano, & V. V Kudriavtsev (Eds.), *Computational technologies for fluid/structural/chemical systems with industrial applications* (pp. 161–168). New York: The American Society of Mechanical Engineers.

Linn, R. R., Reisner, J., Colman, J. J., & Winterkamp, J. L. (2002). Studying wildfire behavior using FIRETEC. *International Journal of Wildland Fire*, *11*(4), 233–246. https://doi.org/10.1071/WF02007

Lorenz, E. N. (1963). Deterministic nonperiodic flow. *Journal of the Atmospheric Sciences*, *20*, 130–141. https://doi.org/10.1175/1520-0469(1963)020<0130:DNF>2.0.CO;2

Lorenz, E. N. (1969). The predictability of a flow which possesses many scales of motion. *Tellus*, *21*(3), 289–307. https://doi.org/10.3402/tellusa.v21i3.10086

Loudermilk, E. L., Achtemeier, G. L., O'Brien, J. J., Hiers, J. K., & Hornsby, B. S. (2014). High-resolution observations of combustion in heterogeneous surface fuels. *International Journal of Wildland Fire*, *23*(7), 1016–1026. https://doi.org/10.1071/WF13160

Mell, W. E., Manzello, S. L., Maranghides, A., Butry, D., & Rehm, R. G. (2010). The wildland – urban interface fire problem – current approaches and research needs. *International Journal of Wildland Fire*, *19*(2), 238–251. https://doi.org/10.1071/WF07131

Mitteroecker, P., Gunz, P., Windhager, S., & Schaefer, K. (2013). A brief review of shape, form, and allometry in geometric morphometrics, with applications to human facial morphology. *Hystrix*, *24*(1), 1–8. https://doi.org/10.4404/hystrix-24.1-6369

Molteni, F., Buizza, R., Palmer, T. N., & Petroliagis, T. (1996). The ECMWF ensemble prediction system: Methodology and validation. *Quarterly Journal of the Royal Meteorological Society*, *122*(529), 73–119. https://doi.org/10.1002/qj.49712252905

National Interagency Fire Center. (2020). Retrieved March 31, 2020, from https://www.nifc.gov/fireInfo/fireInfo_statistics.html

Nelson, R. M. (2003). *Power of the fire – A thermodynamic analysis. In International journal of wildland fire* (Vol. 12, pp. 51–65). CSIRO Publishing. https://doi.org/10.1071/WF02032

10.1029/2020JD033384

O'Brien, J. J., Loudermilk, E. L., Hornsby, B., Hudak, A. T., Bright, B. C., Dickinson, M. B., et al. (2016). High-resolution infrared thermography for capturing wildland fire behaviour: RxCADRE 2012. *International Journal of Wildland Fire*, *25*(1), 62–75. https://doi.org/10.1071/WF14165

Pimont, F., Dupuy, J. L., Caraglio, Y., & Morvan, D. (2009). Effect of vegetation heterogeneity on radiative transfer in forest fires. *International Journal of Wildland Fire*, *18*(5), 536–553. https://doi.org/10.1071/WF07115

Pimont, F., Dupuy, J.-L., Linn, R. R., & Sauer, J. A. (2018). A specific large-scale pressure gradient forcing for computation of realistic 3D wind fields over a canopy at stand scale. *Preprints*, 2018100332. https://doi.org/10.20944/preprints201810.0332.v1

Potter, B. E., (2012). Atmospheric interactions with wildland fire behaviour – I. Basic surface interactions, vertical profiles and synoptic structures. *International Journal of Wildland Fire*, *21*(7), 779–801. https://doi.org/10.1071/WF11128

Prichard, S., Larkin, N., Ottmar, R., French, N., Baker, K., Brown, T., et al. (2019). The fire and smoke model evaluation experiment—a plan for integrated, large fire–atmosphere field campaigns. *Atmosphere*, *10*(2), 66. https://doi.org/10.3390/atmos10020066

Raupach, M. R., Finnigan, J. J., & Brunet, Y. (1996). Coherent eddies and turbulence in vegetation canopies: The mixing-layer analogy. In *Boundary-layer meteorology 25th anniversary* (Vol 78, pp. 351–382). Springer Netherlands. https://doi.org/10.1007/978-94-017-0944-6_15

Reifsnyder, W. E. (1954). *Atmospheric stability and forest fire behavior*. New Haven, CT: Yale University.

Reisner, J., Wynne, S., Margolin, L., & Linn, R. R. (2000). Coupled atmospheric–fire modeling employing the method of averages. *Monthly Weather Review*, *128*, 3683–3691. https://doi.org/10.1175/1520-0493(2001)129<3683:CAFMET>2.0.CO;2

Rothermel, R. C. (1972). *A mathematical model for predicting fire spread in wildland fuels*. Retrieved from https://www.fs.fed.us/rm/pubs_int/int_rp115.pdf

Schweizer, D. W., & Cisneros, R. (2017). Forest fire policy: Change conventional thinking of smoke management to prioritize long-term air quality and public health. *Air Quality, Atmosphere and Health*, *10*(1), 33–36. https://doi.org/10.1007/s11869-016-0405-4

Sivakumar, B., (2004). Chaos theory in geophysics: Past, present and future. *Chaos, Solitons & Fractals*, *19*(2), 441–462. https://doi.org/10.1016/S0960-0779(03)00055-9

Sullivan, A. L. (2009). Wildland surface fire spread modelling, 1990–2007. 1: Physical and quasi-physical models. *International Journal of Wildland Fire*, *18*, 349–368. https://doi.org/10.1071/WF06143

Sun, R., Krueger, S. K., Jenkins, M. A., Zulauf, M. A., & Charney, J. J. (2009). The importance of fire–atmosphere coupling and boundary-layer turbulence to wildfire spread. *International Journal of Wildland Fire*, *18*(1), 50–60. https://doi.org/10.1071/WF07072

Thaxton, J. M., & Platt, W. J. (2006). Small-scale fuel variation alters fire intensity and shrub abundance in a pine savanna. *Ecology*, *87*(5), 1331–1337. https://doi.org/10.1890/0012-9658

Thompson, P. D. (1957). Uncertainty of initial state as a factor in the predictability of large scale atmospheric flow patterns. *Tellus*, *9*(3), 275–295. https://doi.org/10.1111/j.2153-3490.1957.tb01885.x

Tribbia, J. J., & Baumhefner, D. P. (2004). Scale interactions and atmospheric predictability: An updated perspective. *Monthly Weather Review*, *132*(3), 703–713. https://doi.org/10.1175/1520-0493

Viscosi, V., & Cardini, A. (2011). Leaf morphology, taxonomy and geometric morphometrics: A simplified protocol for beginners. *PloS One*, *6*(10), e25630. https://doi.org/10.1371/journal.pone.0025630

Ward, D. E., & Lamb, R. C. (1970). Prescribed burning and air quality – current research in the south. In *Proceedings of the 10th Tall Timbers fire ecology conference* (pp. 129–140). Tallahassee, FL: Tall Timbers.

Whitten, J. L., & Martin, E. S. (2019). Icelandic pit chains as planetary analogs: Using morphologic measurements of pit chains to determine regolith thickness. *Journal of Geophysical Research: Planets*, *124*(11), 2983–2999. https://doi.org/10.1029/2019JE006099

Wonkka, C. L., Rogers, W. E., & Kreuter, U. P. (2015). Legal barriers to effective ecosystem management: Exploring linkages between liability, regulations, and prescribed fire. *Ecological Applications*, *25*(8), 2382–2393. https://doi.org/10.1890/14-1791.1

Yedinak, K., Strand, E., Hiers, J., & Varner, J. (2018). Embracing complexity to advance the science of wildland fire behavior. *Fire*, *1*(2), 20. https://doi.org/10.3390/fire1020020

Zeng, X., Pielke, R. A., Eykholt, R., Zeng, X., Pielke, R. A., & Eykholt, R. (1993). Chaos theory and its applications to the atmosphere. *Bulletin of the American Meteorological Society*, *74*(4), 631–644. https://doi.org/10.1175/1520-0477

Zhao, W., Liu, J., & Bicknell, R. D. C. (2020). Geometric morphometric assessment of guanshan trilobites (Yunnan province, china) reveals a limited diversity of palaeolenid taxa. *Palaeontologia Electronica*, *23*(2), 1–15. https://doi.org/10.26879/1062